



ICE THERMAL LOADS AGAINST WALLS OF
WATER RESERVOIRS

Pauli Jumppanen
Associate Professor

Helsinki University
of Technology

1. INTRODUCTION

It is well known that changes of air temperature cause appreciable ice pressures upon structures located in or around uniform ice fields. Such structures are water reservoirs of different types, water troughs of channels, harbour piers, tanks in water, and others of the same kind.

The usual method used in the evaluation of maximal ice loads in different circumstances consists in doing measurements in nature [8] or model tests in laboratory [7], [9]. Some analysing methods based on the knowledge of the thermo-mechanical properties of ice has also been put forth. These properties are determinable e.g. by doing constant strain rate tests with ice samples at various temperatures. By the use of the measured stress-time curves, it is then possible to solve the stresses in ice as a function of strain or strain rate [2], [5].

In this paper, an alternative technique is considered for the evaluation of the thermal stresses in ice cover and

of the ice loads on vertical structures. At first, a thermorheologic model is formed for ice by the use of one-dimensional constant creep tests at different temperatures. Although constant strain or constant strain rate tests are more convenient from the physical aspect, in practice the creep tests are more easy to perform. Furthermore, a procedure is presented for the evaluation of material parameters in the rheologic model. Numerical solutions are effected for two different types of ice by the use of creep tests made for this purpose. Finally, a numerical technique is proposed for the determination of ice pressures exerted by an ice sheet the thermal expansion of which is obstructed by vertical walls. The technique is also applied to the treatment of some usual problems in practice.

2. THERMORHEOLOGIC MODEL FOR ICE

The two-dimensional constitutive equation of a linear isotropic thermoviscoelastic material in a constant temperature θ is expressible in terms of the known functional [3]

$$E = J_0 I + \int_0^t [J_1(t-\tau, \theta) I \operatorname{tr} \dot{S} + J_2(t-\tau, \theta) \dot{S}] d\tau \quad (1)$$

Here, E and S are strain and stress matrices

$$E = \begin{bmatrix} \epsilon_x & \frac{1}{2}\gamma \\ \frac{1}{2}\gamma & \epsilon_y \end{bmatrix}, \quad S = \begin{bmatrix} \sigma_x & \tau \\ \tau & \sigma_y \end{bmatrix}, \quad (2)$$

J_0 , J_1 , and J_2 the response (creep) functions of the material, and τ the time variable on the interval $[0, t]$. Furthermore,

I is the unit matrix, $(\dot{})$ means the first time derivative (d/dt), and then

$$\text{tr} \dot{S} = \dot{\sigma}_x + \dot{\sigma}_y \quad (3)$$

If the first term in Equation (1), which means e.g. a thermal expansion, is omitted to write, separate strain components acquire forms

$$\begin{aligned} \epsilon_x &= \int_0^t [J_1(\dot{\sigma}_x + \dot{\sigma}_y) + J_2 \dot{\sigma}_x] d\tau, \\ \epsilon_y &= \int_0^t [J_1(\dot{\sigma}_x + \dot{\sigma}_y) + J_2 \dot{\sigma}_y] d\tau, \\ \gamma &= 2 \int_0^t J_2 \dot{\tau} d\tau. \end{aligned} \quad (4)$$

The comparison between Equation (1) and the corresponding elasticity equation,

$$E = -\frac{\nu}{E} I \text{ tr} S + \frac{1}{2G} S,$$

leads to the interpretation that J_1 means the time variation of the elasticity modulus ν/E and, correspondingly, J_2 the time variation of the modulus $1/2G$.

In the later treatment, two special cases of Equations (1) and (4) are needed.

a. One-dimensional case $\sigma_x = \sigma$, $\sigma_y = \tau = 0$.

Formulae (4) give:

$$\epsilon_x = \int_0^t (J_1 + J_2) \dot{\sigma} d\tau = \int_0^t J(t-\tau, \theta) \dot{\sigma}(\tau) d\tau, \quad (5)$$

$$\epsilon_y = \int_0^t J_1 \dot{\sigma} d\tau = v(\theta) \int_0^t J(t-\tau, \theta) \dot{\sigma}(\tau) d\tau, \quad (5)$$

$$\gamma = 0$$

J means here the inverse value of the modulus of elasticity E as function of time. The formula of ϵ_y involves that in the deformation process the Poissons ratio v is dependent only on temperature θ (but not on time). This is a suitable assumption for ice in accord with a number of investigators [1], [6].

$$b. \quad \sigma_x = \sigma_y = \sigma, \quad \tau = 0.$$

This case leads to the expressions of strains

$$\epsilon_x = \epsilon_y = \int_0^t (2J_1 + J_2) \dot{\sigma} d\tau = [1 - v(\theta)] \int_0^t J(t-\tau, \theta) \dot{\sigma}(\tau) d\tau, \quad (6)$$

$$\gamma = 0,$$

where the assumption $v = v(\theta)$ is also made.

The rheologic equations presented above are valid only at constant remperatures. To solve ice pressure problems in variable temperatures, however, the temperature dependence of the stress-strain law (1) is to be considered. The most simple method of representing this temperature dependence affords the so-called shifting hypothesis which is the basic postulate of thermorheologically simple materials. This approach has been widely used to describe creep or stress-relaxation of metals at high temperatures [10] and of various types of polymers [4]. In this connection, the shifting phenomenon is representable in the following way.

If θ_0 is a reference temperature, and it is denoted

$$J(t-\tau, \theta_0) = J(t-\tau), \quad (7)$$

at an other constant temperature $\theta > \theta_0$ the creep function is expressible in the form

$$J(t-\tau, \bar{\theta}) = \kappa_0 \bar{\theta} + J[(t-\tau)\kappa(\bar{\theta})], \quad (8)$$

where $\bar{\theta} = \theta - \theta_0$. The first term $\kappa_0 \bar{\theta}$ means a vertical shift of the creep function along the J -axis, and $\kappa(\bar{\theta})$ causes a horizontal shift of J along the log-time axis (Fig. 1). $\kappa(\bar{\theta})$ is the so-called shift function which depends only on temperature and obeys the relations

$$\kappa(0) = 1, \quad \frac{d\kappa(\bar{\theta})}{d\bar{\theta}} > 0. \quad (9)$$

Furthermore, at variable temperatures $\theta(t)$ the creep modulus can be written to the form

$$J(t-\tau, \bar{\theta}) = \kappa_0 \bar{\theta}(t) + J[\phi(t) - \phi(\tau)], \quad (10)$$

where

$$\begin{aligned} \bar{\theta}(t) &= \theta(t) - \theta_0, \\ \phi(t) &= \int_0^t \kappa[\bar{\theta}(\tau)] d\tau. \end{aligned} \quad (11)$$

By virtue of Equation (10), the rheologic equation (6) can now be replaced by the thermorheologic model

$$\begin{aligned} \epsilon_x(t, \bar{\theta}) &= [(1 - \nu(\bar{\theta}))\{\kappa_0 \bar{\theta}(t) + \\ &+ \int_0^t J[\phi(t) - \phi(\tau)] \dot{\sigma}(\tau) d\tau\}. \end{aligned} \quad (12)$$

If a rheologic equation is used in the more general form (1), different shift functions are to be considered for the both moduli J_1 and J_2 .

3. CREEP TESTS AND MATERIAL PARAMETERS

To consider suitable creep functions for ice, about 50 creep tests were performed in the Cold Laboratory of the Civil Engineering Department, at Helsinki University of Technology. Two types of fresh water were studied:

- Columnar grained ice made of tap water (not boiled) in the laboratory (the density $\rho = 0.87 - 0.91 \text{ g/cm}^3$)
- Columnar grained ice taken from ice cover at Saima channel (between the Lake Saima and the Baltic Sea) (the density $\rho = 0.92 \text{ g/cm}^3$).

Cylindrical samples bored out from ice blocks were orientated horizontally in the ice cover and parallel to the c-axis of crystals. The dimensions of samples were: height $\approx 150 \text{ mm}$, diameter $\approx 90 \text{ mm}$. The test temperatures were -2 , -5 , -12 , and -25°C . To get light on the nonlinearity of creep behaviour with respect to effective stress, creep tests on different stress levels 3 kp/cm^2 , 7 kp/cm^2 , and 12 kp/cm^2 were also made. The strains were automatically registered by a xy-recorder from the movements of a typical creep testing machine. The testing time was 24 hours.

Some typical creep curves are shown in Figure 2. The tests indicated that the creep phenomenon is markedly accelerated by the increasing temperature. The experiments under stress 7 kp/cm^2 showed weak nonlinearity and under stress 12 kp/cm^2 strong nonlinearity of creep values regarding to the stress. In the latter case, the tertiary phase of creep began in some hours and led in the most cases to the breaking before the end of the experiment. On this basis, only linear creep

functions are considered in this study by the use of tests on the stress levels 3 and 7 kp/cm².

Of some creep functions studied, expressions

$$J(t) = a + bt^n, \quad (13)$$

$$J(t) = a - be^{-\alpha t} - ce^{-\beta t} \quad (14)$$

gave the best agreement with the individual test results. In the following, however, only Equation (13) is applied.

The corresponding temperature dependent creep equation is in accord with Formula (8)

$$J(t, \bar{\theta}) = a(\bar{\theta}) + b(\bar{\theta})t^n, \quad (15)$$

where

$$\begin{aligned} a(\bar{\theta}) &= a + \kappa_0 \bar{\theta}, \\ b(\bar{\theta}) &= b\kappa(\bar{\theta})^n. \end{aligned} \quad (16)$$

The shifting character of Equation (15) does not change if the parameter $b\kappa(\bar{\theta})^n$ is replaced by an arbitrary function $b(\bar{\theta})$. The values of all the parameters a , b , and n are also dependent on grain diameters, orientation of grains, salt content, and on other internal variables of ice. Anyway, these dependences are not considered in this study.

For the evaluation of the temperature dependence of the parameters $a(\bar{\theta})$ and $b(\bar{\theta})$, the constants a , b , and n in Equation (13) have been at first solved for measured creep curves at different temperatures (e.g. Fig. 2). This has been effected by the employment of the least-squares method together with an iterative procedure. For estimation of the applicability of the applied creep model, the mean dispersal

$$S = \left\{ \frac{1}{m-1} \sum_{i=1}^m [\bar{J}(t_i, \bar{\theta}) - J(t_i)]^2 \right\}^{1/2} \quad (17)$$

has been computed for all the solutions. Here, $\bar{J}(t_i, \theta)$ is the measured value of creep, and $J(t_i)$ the value of the actual regression curve (13) at instant t_i . The number of time points (m) has been 30 in every computation.

The calculations showed that the values obtained for the parameter n are quite independent on the temperature (Fig. 3), and that the fixed value

$$n = 0.3 \quad (18)$$

can be chosen. Thereafter, the constants a and b have been calculated anew by applying this fixed value of n . The dispersal S (17) varied now from $0.01^\circ/\infty$ to $0.1^\circ/\infty$, while the maximal strains in creep curves were $3 - 10^\circ/\infty$. This holds in those cases where cracks, local breakings, or tertiary creep did not appear during the deformation process.

By the use of the values computed for a and b at different temperatures, the following temperature dependences can be expressed for the creep moduli (16).

$$a(\bar{\theta}) = (1.17 + 0.036 \bar{\theta}) \cdot 10^{-5} [\text{cm}^2/\text{kp}], \quad (19)$$

$$b(\bar{\theta}) = (24.5 + 0.5 \bar{\theta}) \cdot 10^{-5} [\text{cm}^2/\text{kp}] \text{ (tap water ice)} \quad (20)$$

$$b(\bar{\theta}) = (12 + 0.25 \bar{\theta}) \cdot 10^{-5} [\text{cm}^2/\text{kp}] \text{ (Saima Channel ice)}. \quad (21)$$

In these expressions,

$$\theta_0 = -25^\circ\text{C}, \quad \bar{\theta} = \theta - \theta_0, \quad 0^\circ\text{C} > \theta \geq -25^\circ\text{C} \quad (22)$$

Equation (19) holds both the ice types investigated with accuracy which corresponds to the accuracy of the used regression model (15). The value of $b(\bar{\theta})$ is quite different for tap water ice and Saima Channel ice. This is probably caused by the air content of tap water ice (density $0.87 - 0.91$), and by the fact that Saima Channel ice had earlier been loaded

by changes temperature inside the ice cover, although in practice it was free of initial stresses in the creep tests.

Quite a great dispersion, usual for ice tests, appeared especially in the values of b (Fig. 4). Therefore, only the linear temperature dependences (20) and (21) have been given for it, and the form of the shift function $\kappa(\bar{\theta})$ has not been considered separately. However, the rheologic model used is not very sensible for the variation of $b(\bar{\theta})$. If instead of Equation (20) formula $b(\bar{\theta}) = (20.5 + 0.5 \bar{\theta}) \cdot 10^{-5}$ is used (dotted line in Fig. 4), only 5 - 3 % higher ice pressures are obtained in the later examples.

The value of Poissons ratio has not been studied in this work. In accord with the measurements of Bogorodskii [1], the expression

$$\nu(\theta) = 0.3 + 0.004 \bar{\theta} \quad (23)$$

is valid on the temperature range (22).

4. SOLUTION OF SOME SIMPLE ICE PRESSURE PROBLEMS

In the following, the thermorheologic model given through Equations (5) or (6), (19), (20) or (21), and (23) is applied to the evaluation of ice pressures, which the temperature changes cause against walls of some types of hydraulic structures. If the thermal expansion of an ice sheet (parallel to zy -plane) is restricted by an vertical wall, horizontal normal stresses arise inside the ice cover. These are considerable smaller than the corresponding elastic stresses because of the stress-relaxation during the temper-

ature change. As the temperature varies at different depths z inside ice, also variable stresses occur as a function of z .

In the following examples, the ice pressures caused by a homogeneous change of temperature in an ice sheet of unit thickness are solved in some simple cases, where the corresponding elasticity solutions are known. If the temperature inside the ice cover varies only as a function of z , $\theta = \theta(z)$, the pressures at different depths can be solved separately, and then the total ice loads against walls of structures can be determined. This procedure neglects, however, the influence of the elastic winklerian foundation in bending of the ice plate. Nevertheless, the measurements performed at Saima Channel (winter 1972-73) showed that the ice pressures and the corresponding temperature changes at different depths inside the ice cover correspond very good to each others (Fig. 9), and satisfactory results are obtainable by the use of the method presented.

Cylindrical water reservoir

The studied structure with the used notations is presented in Figure 5. The strains of the ice sheet caused by temperature change are given by the equation

$$\epsilon(t) = \alpha(\theta)\bar{\theta}(t). \quad (24)$$

$\alpha(\theta)$ is the expansion coefficient for which a constant value $6 \cdot 10^{-5}/^{\circ}\text{C}$ is taken. The pressure p on the surrounding cylinder causes normal stresses $\sigma_r(r, \phi) = \sigma_{\phi}(r, \phi) = p$ in the circular ice sheet. By the use of Equations (6) and (24), the expres-

sion,

$$u(R,t) = \alpha R \bar{\theta}(t) - R[1-\nu(\bar{\theta})] \int_0^t J(t-\tau, \bar{\theta}) \dot{p}(\tau) d\tau, \quad (25)$$

can be written for the radial displacement of the edge of the ice plate.

The reservoir is approximately considered to be a long circular cylindrical shell. For a line load q uniformly distributed along a circular section, the maximal displacement of the shell is in accord with Timoshenko [11]

$$u'(t) = \alpha' R \bar{\theta}(t) + A p(t), \quad (26)$$

where

$$A = \frac{R^2}{E'h} (1 - e^{-\beta b} \cos \beta b), \quad \beta = \sqrt{\frac{3(1-\nu'^2)}{R^2 h^2}} \quad (27)$$

Here, E' and ν' are the elasticity moduli and α' the thermal expansion coefficient of the material of the shell.

The compatibility condition between the displacements (25) and (26),

$$u(R,t) = u'(t),$$

leads to the equation

$$(\alpha - \alpha') R \bar{\theta}(t) - A p(t) - R[1-\nu(\bar{\theta})] \int_0^t J(t-\tau, \bar{\theta}) \dot{p}(\tau) d\tau = 0 \quad (28)$$

for the determination of the ice pressure $p(t)$.

In the numerical treatment of Equation (28), the segment $[0, t]$ is divided into n increments of equal length Δt , and the time rates of stress are expressed by the difference formula

$$\dot{p}(i\Delta t) = \frac{p[(i+1)\Delta t] - p[(i-1)\Delta t]}{2\Delta t}, \quad i = 0, 1, 2, \dots, n \quad (29)$$

Furthermore, the values of $p(t)$ are calculated stepwise at

all the instants $0, \Delta t, 2\Delta t, \dots, n\Delta t$ by the application of the trapezoidal rule in the numerical integration.

In the calculations, the time increment Δt was 6 minutes. The temperature was assumed to change linearly from -20°C to -0°C or from -10°C to -0°C , and the warming time was 4, 12, or 24 hours. The solutions were also effected for the tap water ice (Eq. (19), (20), (23)) and for the Saima Channel ice (Eq. (19), (21), (23)). The wall of the concrete cylinder was 20 cm or 50 cm thick, and also the case of infinitely rigid wall was treated. In the calculation of the displacement u' (26), the ice sheet was assumed to be 60 cm thick, the thermal expansion coefficient $\alpha' = 0$, and the Poisson's ratio of concrete $\nu' = 1/6$.

Some pressure-time curves are shown in Figure 6. The values of maximal pressures obtained in all the computed cases are presented in the following table 1.

Table 1. Maximal ice pressures on cylindrical water reservoir

Type of ice	R [cm]	h [cm]	E' [kp/cm ²]	ν'	Warming [°C]	Warming time [h]	Pmax [kp/cm ²]
a	arbitrary		∞	1/6	20 \rightarrow 0	4	4.56
b	arbitrary		∞	1/6	20 \rightarrow 0	4	8.82
a	arbitrary		∞	1/6	20 \rightarrow 0	12	3.32
b	arbitrary		∞	1/6	20 \rightarrow 0	12	6.47
a	arbitrary		∞	1/6	20 \rightarrow 0	24	2.71
b	arbitrary		∞	1/6	20 \rightarrow 0	24	5.31
a	arbitrary		∞	1/6	10 \rightarrow 0	12	1.60
b	arbitrary		∞	1/6	10 \rightarrow 0	12	3.11
b	1000	20	$3 \cdot 10^5$	1/6	20 \rightarrow 0	12	3.64
b	1000	50	$3 \cdot 10^5$	1/6	20 \rightarrow 0	12	4.95

a = tap water ice, b = Saima Channel ice

If the walls of the reservoir are assumed to be infinitely rigid, a homogeneous temperature rise in the area of the ice cover gives cause to constant normal stresses $\sigma_x(t) = \sigma_y(t)$ and to uniformly distributed pressure $p(t)$ against all the walls, although the relation c/d varies (Fig. 7). By this means, Equation (28) is valid also in this case, if the term $Ap(t)$ is neglected. This is effected by setting $E' = \infty$ in the formula of A (27), and then the values of the ice pressure in Table 1 hold in this parts also for right-angled water reservoirs.

Long channel trough

This case can be easily solved by the application of the one-dimensional case (5) under assumption $v(\theta) \equiv 0$. If Formula (5) of ϵ_x is used instead of Formula (6), in the case of infinitely rigid walls the equation of solving takes the form (for arbitrary value of c)

$$\alpha \bar{\theta}(t) - \int_0^t J(t-\tau, \bar{\theta}) \dot{p}(\tau) d\tau = 0. \quad (30)$$

It can also be treated as a special case of Equation (28). Some results obtained in calculations, by the use of the rheologic model of Saima Channel ice, is given in Table 2.

Table 2. Maximal ice pressures against walls of a long channel trough.

Warming [$^{\circ}\text{C}$]	Warming time [h]	P_{\max} [kp/cm 2]
20 \rightarrow 0	12	3.74
20 \rightarrow 0	24	3.07
10 \rightarrow 0	12	1.84
10 \rightarrow 0	24	1.51

Continuous measurements of air temperature changes, as well as changes of temperature and ice pressure at different depths inside ice, has been performed at Saima Channel during the winter 1972-73. The variation of the temperature and the pressure at the depth of 8 cm inside ice is shown from a period of 28 hours in Figure 9. By the use of the measured temperature variation and the rheologic model of Saima Channel ice, the ice pressure variation is solved from Equation (30). Satisfactory agreement is to be seen in Figure 9 between the maximal values of the measured and calculated pressures.

Ice pressure problems of other types of water reservoirs and basins can also be treated by the method presented applying known analytic elasticity solutions of the plate and the reservoir in question. In the cases where the analytic solutions are not known, the finite difference method of the finite element method can be used.

The values of maximal ice pressures measured in nature (e.g. [7], [8]) correspond in the class of magnitude the values obtained in this investigation. Of the ice types studied Saima Channel ice seems to give more realistic values for the ice pressure. Nevertheless, a great number of creep and stress relaxation tests should be performed to obtain reliable rheologic models for different ice types.

ACKNOWLEDGEMENTS

This work was financially supported by Tekniikan Edistämissäätiö. The ice pressure measurements were performed

of an order of Administration of Public Works and Water Buildings. The author is indebted to Mr Seppo Hakari for remarkable help in the experiments, and Mr Erkki Leppävuori in the computer applications.

ABSTRACT

The biggest ice forces concentrated upon structures in or around continuous ice fields are caused by the temperature changes. This paper presents a technique which is applicable in the evaluation of ice thermal stresses against walls of different kinds of water reservoirs and of small water basins with nearly homogeneous ice cover.

The technique is based on the theory of creep and stress-relaxation of ice. At first, an one-dimensional creep law is formed for columnar ice perpendicular to the principal axes of columns. This is accomplished doing creep tests with cylindrical ice samples in various constant temperatures (-2°C , -5°C , -12°C , and -25°C) and on different stress levels (3 kp/cm^2 , 7 kp/cm^2 , and 12 kp/cm^2). Among some creep equations considered, the function

$$J(t, \theta) = a(\theta) + b(\theta)t^{n(\theta)}$$

gave the best agreement with test results. Here, a , b , and n are material parameters dependable on temperature (θ) and on different internal variables of ice. The creep law is then generalized to two-dimensional case by introducing a new material constant, Poisson's ratio, which also is dependable on temperature.

The ice cover in water reservoirs or basins is considered as a thin plate, the normal forces of which can be evaluated separately from the bending phenomenon of the plate. If now the temperature changes at different depths inside ice, or the average temperature changes in ice cover, are known, the pressures against walls of water reservoirs can be evaluated

by the use of the theory of stress-relaxation in ice.

In numerical examples water reservoirs of different form of surfaces are treated. In one of them, the influence of the flexibility of walls is taken into account. The numerical results are also compared with the pressures measured at Saima Channel (winter 1973) and with other corresponding measurements found in literature.

REFERENCES

1. Bogorodskii, V.V., Uprugie kharakteristike l'da. Akust. Zhurn. 4 (1958).
2. Drouin, M., Laboratory investigations on ice thermal pressures. Ice Symposium in Leningrad (1972).
3. Eringen, A.C., Mechanics of continua (chapt. 9). Wiley, 1967.
4. Ferry, J.D., Viscoelastic properties of polymers. Wiley 1961.
5. Gold, L.W., Elastic and strength properties of fresh-water ice. NCR Canada Techn. Paper No. 283 (1968).
6. Lavrov, V.V., Deformation and strength of ice (Leningrad 1969). Israel Progr. Sci. Transl., Jerusalem 1971.
7. Löfquist, B., Studies of the temperature variations (Symposium of Ice Pressure against Dams). Trans. Soc. Civ. Eng. 119 (1954).
8. Monfore, G.E., Experimental investigations by the Bureau of Reclamation (Symposium of Ice Pressure against Dams). Trans. Soc. Civ. Eng. 119 (1954).
9. Nuttal, J. / Gold, L.W., Model study of ice pressures. NCR Canada Research Paper No. 378 (1968).
10. Sherby, O.D. / Dorn, J.E., J. of Metals (pp. 324...330) 5. (1953).
11. Timoshenko, S. / Woinowsky-Krieger, S., Theory of plates and shells. McCraw-Hill 1959.

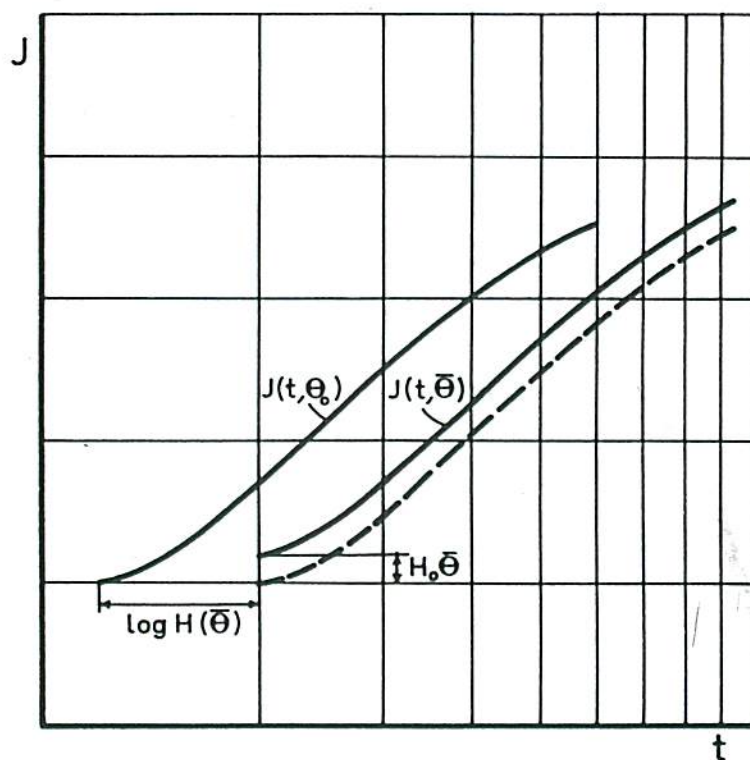


Figure 1. Effect of change in temperature on the creep function.

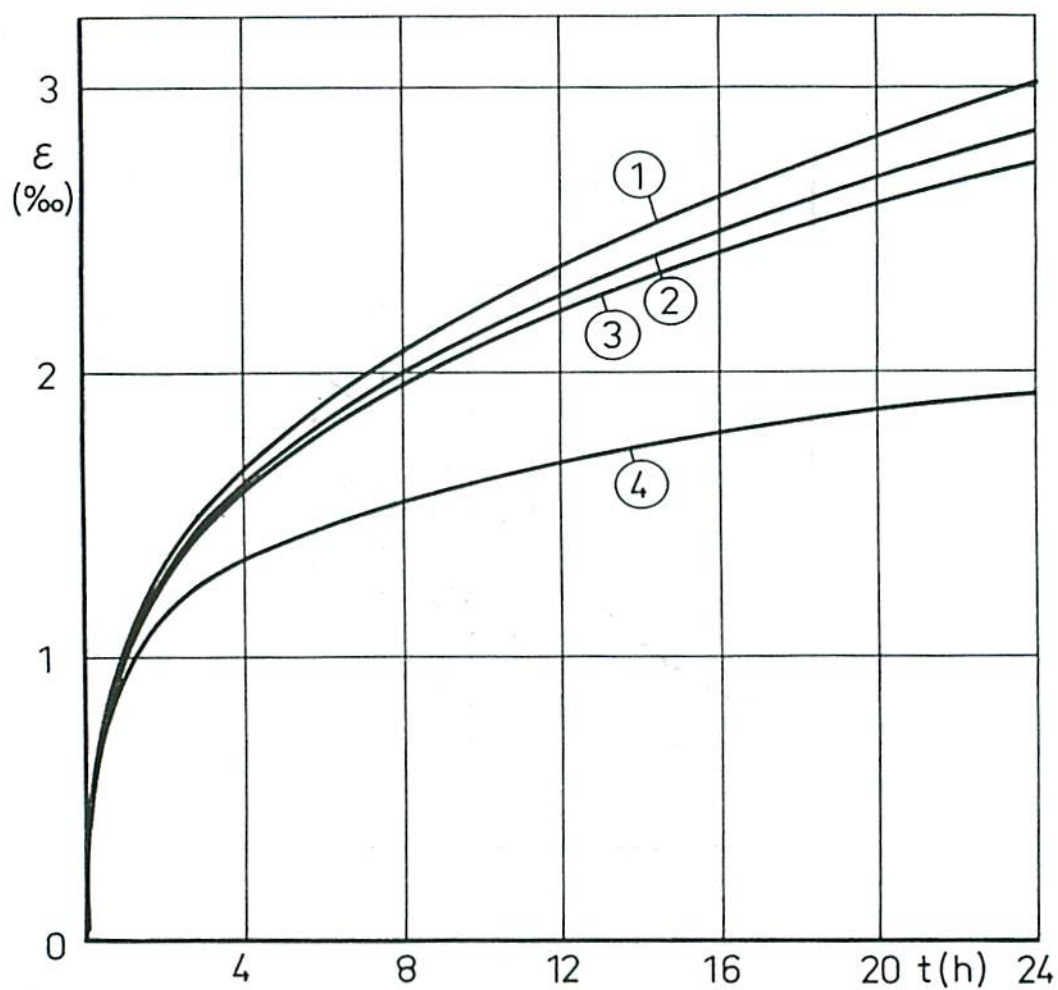


Figure 2. Creep curves of tap water ice at different temperatures:
 4) $\theta = -25^{\circ}\text{C}$, $\sigma = 3,2 \text{ kp/cm}^2$, 3) $\theta = -12$, $\sigma = 3,16$,
 2) $\theta = -5$, $\sigma = 3,21$, 1) $\theta = -2$, $\sigma = 3,08$.

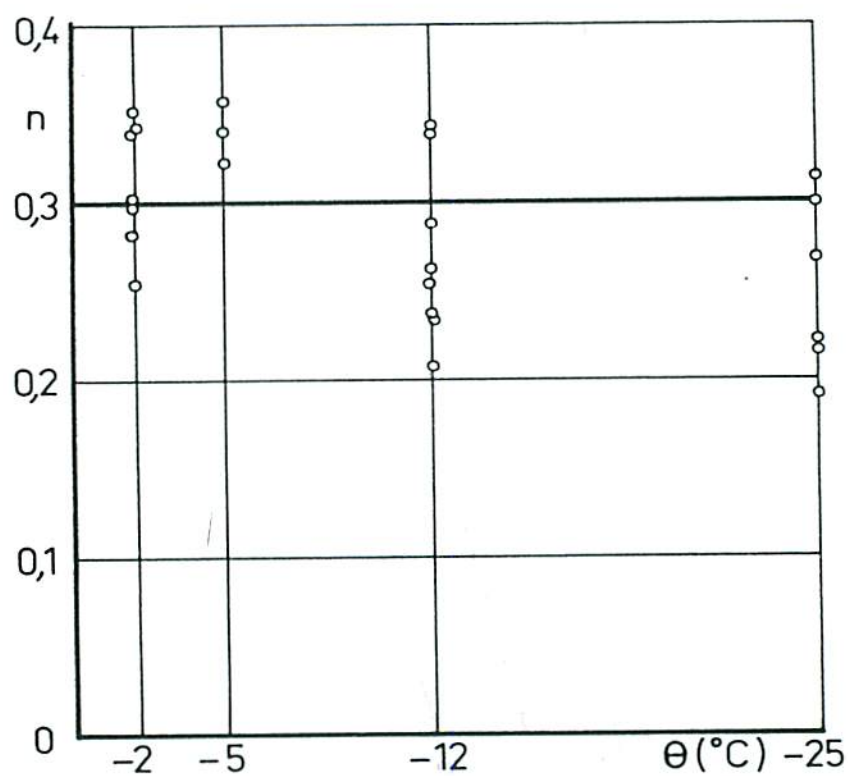


Figure 3. Values of the exponent n at different temperatures.

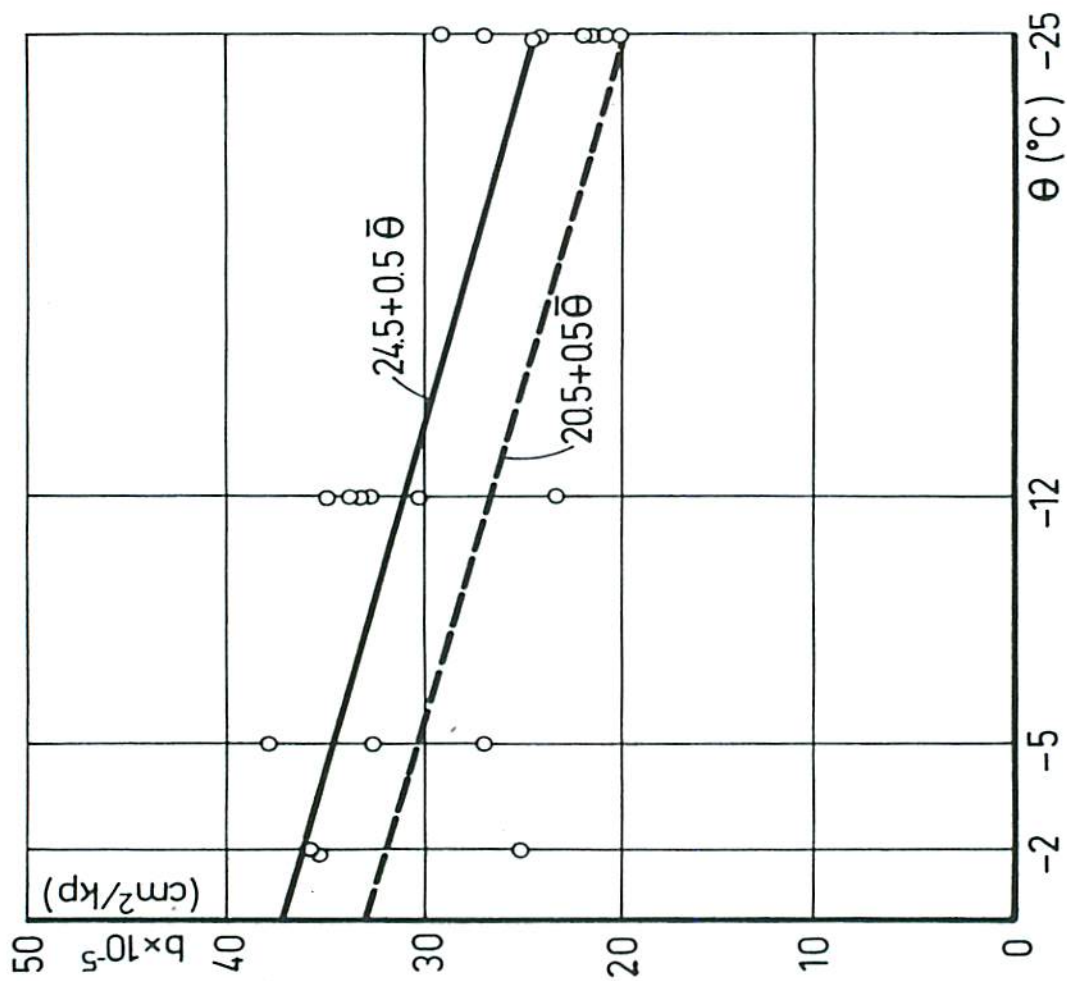


Figure 4. Values of the material parameter b at different temperatures.

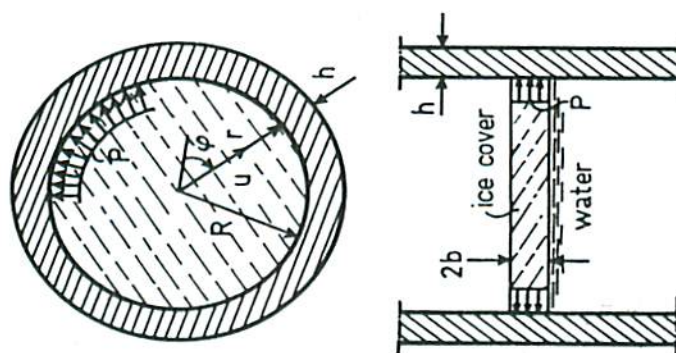


Figure 5. Circular water reservoir.

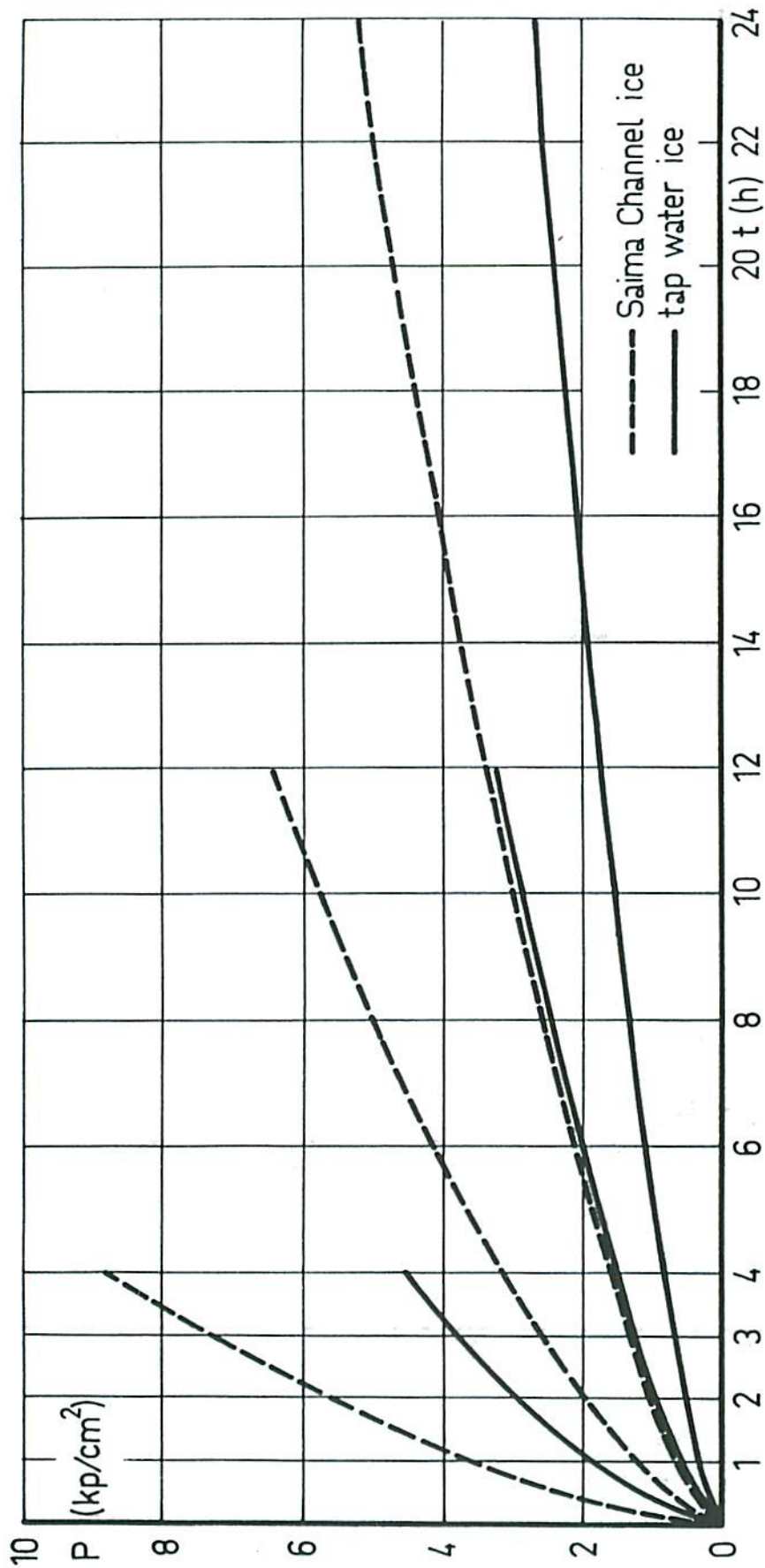


Figure 6. Ice pressure variation in the stiff circular water reservoir, when the temperature of ice rises linearly from -20°C to -0°C in 4, 12, and 24 hours.

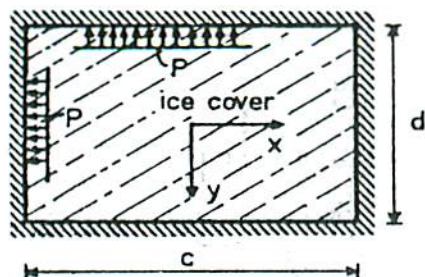


Figure 7. Water reservoir with right-angled surface.

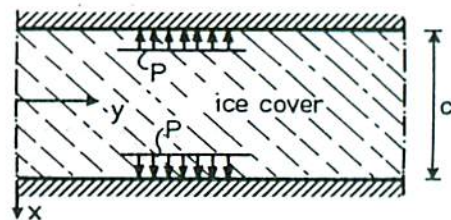


Figure 8. Long channel trough.

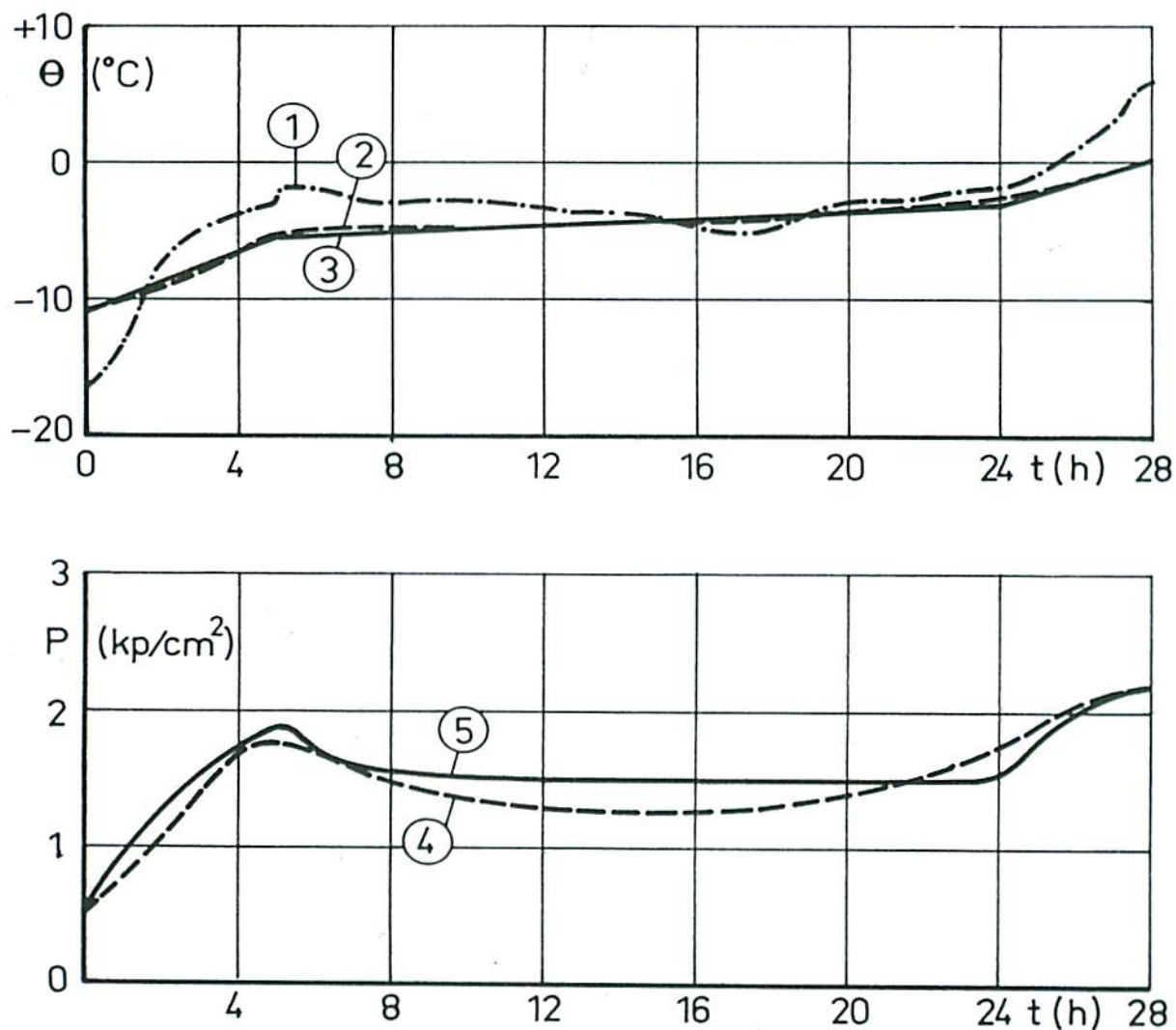


Figure 9. Values of ice pressure and temperature at Saima Channel: 1) air temperature, 2) ice temperature at depth 8 cm, 3) approximated ice temperature in calculations, 4) measured ice pressure at depth 8 cm inside ice, 5) calculated ice pressure.